Spatial dependence of banded chorus intensity near the magnetic equator

N. Haque,[1] U. S. Inan,[1,2] T. F. Bell,[1] and J. S. Pickett[3]

Received 6 July 2012; revised 28 July 2012; accepted 31 July 2012; published 12 September 2012.

[1] Data from 12 different Cluster orbits containing banded chorus emissions, with observations from 22 different events spread across the four Cluster spacecraft, are used to show the spatial dependence of banded chorus intensity near the magnetic equator under conditions of moderate magnetic disturbance ($K_p \leq 5$). The intensities for upper band (UB) and lower band (LB) chorus were manually determined from frequency-time spectrograms generated from WBD data. Out of the 22 events, 5 of the spacecraft observations showed a complete absence of chorus emissions within 0.5° of the magnetic equator. The intensity, I, of the chorus emissions generally increased exponentially with distance, z, away from the magnetic equator according to the relation $I = I_o e^{\alpha z}$, where α is the spatial growth factor. The exponential distribution of α provides a new boundary condition for consideration in current and future chorus generation models. **Citation:** Haque, N., U. S. Inan, T. F. Bell, and J. S. Pickett (2012), Spatial dependence of banded chorus intensity near the magnetic equator, *Geophys. Res. Lett.*, *39*, L17103, doi:10.1029/2012GL052929.

1. Introduction

[2] Whistler mode chorus waves are intense discrete emissions that range in frequency from a few hundred Hz to several kHz. These naturally occurring electromagnetic plasma waves are generated near the magnetic equator outside the plasmasphere [*Dunckel and Helliwell*, 1969; *Russell et al.*, 1970]. Chorus emissions are often observed in a configuration known as banded chorus, with one band above $f_{ce}/2$, known as the upper band (UB), and one band below $f_{ce}/2$, known as the lower band (LB), where f_{ce} is the electron gyrofrequency [*Tsurutani and Smith*, 1974].

[3] Interactions between chorus emissions and radiation belt electrons with energies of 10 to 100 keV during and after geomagnetic storms can result in energy diffusion and thus contribute to the acceleration of these electrons to MeV energies [*Horne and Thorne*, 1998; *Horne et al.*, 2005a, 2005b; *Shprits et al.*, 2006; *Summers et al.*, 2007a, 2007b]. Previous studies have generally concerned the dependence of chorus intensity on substorm activity [e.g., *Tsurutani and Smith*, 1974]. *Thorne et al.* [1974] studied ELF dawn chorus emissions, with frequency range 100 to 1000 Hz, concluding that chorus increases in intensity during a substorm and is most intense for $L > 4$. Many statistical surveys of chorus emissions have been done in the past [e.g., *Tsurutani and Smith*, 1977; *Koons and Roeder*, 1990; *Parrot and Gaye*, 1994]. More recently, *Meredith et al.* [2001] did a detailed study of chorus intensities, using CRRES measurements, for both upper and lower band chorus as a function of L-shell and MLT. They found that chorus within 15° of the equator had the largest intensities between 23.0 and 13.0 hours of magnetic local time (MLT) for $L = 3 - 7$.

[4] These early studies mainly focus on the L-shell and magnetic activity dependence of chorus intensity. In contrast, there has been little work carried out concerning the intensity of chorus in the source region close to the magnetic equator. Since chorus is believed to be generated near the magnetic equatorial plane [*LeDocq et al.*, 1998], it is important to study the spatial dependence of chorus intensity as a function of magnetic latitude, λ, in order to better understand the chorus generation process.

[5] The present study aims to determine the spatial dependence of chorus intensity near the magnetic equator by analyzing 12 Cluster orbits containing banded chorus emissions, with observations from a total of 22 different events spread across the four Cluster spacecraft. These orbits are from the years 2003, 2004, and 2006. The trajectory of Cluster for these events is shown in a meridional plane projection in Figure 1a. The banded chorus events were chosen to include the source region, roughly defined as magnetic latitudes within 5° of the magnetic equator for this study. The magnetic equator is determined using the multipoint determination method described in *Santolík et al.* [2009]. As there are data from multiple spacecraft for each orbit, the trajectories appear to be clustered together. In addition, the 22 events were chosen such that the K_p index at the time was less than 5, with an average K_p of 3.15, indicating there was low to moderate storm-level geomagnetic activity and that the location of the magnetic equator could be reasonably determined [*Santolík et al.*, 2009]. The spacecraft sample L-shells in the range 3.6 to 4.9 and MLT in the range 1.3 to 15.0 hours, seen in Figure 1b.

2. Chorus Intensity as a Function of Magnetic Latitude

[6] The E field frequency-time spectrogram of WBD data [*Gurnett et al.*, 2001] in Figure 2a shows Cluster 3 observations of banded chorus on October 31, 2003, 23:01:02–23:07:54 UT for magnetic latitudes −3° to 0°, MLT of 8.42 h, and K_p index of 4+. The WBD instrument cycles every 52 s, recording data from the electric antenna for 42 s and data from the magnetic antenna for 10 s. For all of the

[1]Space, Telecommunications, and Radioscience Laboratory, Stanford University, Stanford, California, USA.
[2]Electrical Engineering Department, Koc University, Istanbul, Turkey.
[3]Department of Physics and Astronomy, University of Iowa, Iowa City, Iowa, USA.

Corresponding author: N. Haque, Space, Telecommunications, and Radioscience Laboratory, Stanford University, 350 Serra Mall, Stanford, CA 94305, USA. (naoshin@stanford.edu)

0094-8276/12/2012GL052929

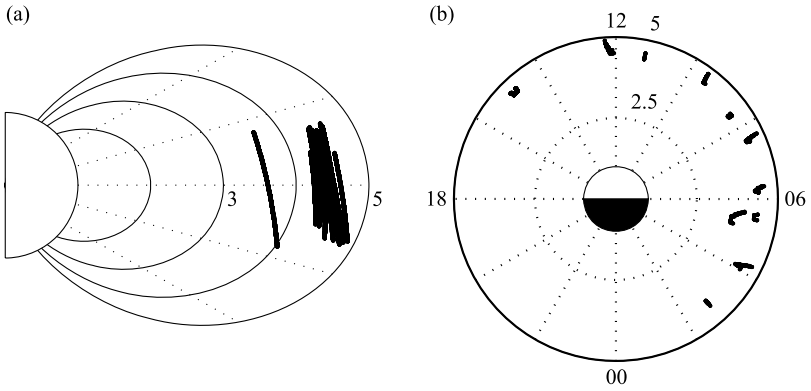

Figure 1. (a) Trajectory of the Cluster spacecraft in a meridional plane projection for the 12 orbits containing banded chorus emissions. The dashed lines represent magnetic latitude increments of 15°, while the solid lines represent dipole *L*-shell increments of 1 R_E. (b) Distribution of MLT and *L*-shells. Each concentric circle represents an increase in *L*-shell by 1 R_E, while each sector represents an increment in MLT by 2 h.

spectrograms in this paper, the data from the electric antenna have been dilated to fill the 10 s data gap during which the magnetic antenna is recorded. The spectrogram in Figure 2a shows the two distinct bands of chorus separated by an emission gap at $f_{ce}/2$, indicated by the white line. The magnetic equator is determined to be at $\lambda_{eq} = -0.55°$ using the multipoint method. Though the upper and lower bands of chorus are not absent at the magnetic equator, the intensity of the emissions appears to be much weaker in this region and also appears to increase with distance away from the magnetic equator.

[7] The values of the average intensities of the upper and lower chorus bands were manually determined from frequency-time spectrograms, which were divided into 1-minute intervals. For each 10 ms time bin, the average intensity was calculated by integrating the wave spectral density ($V^2m^{-2}Hz^{-1}$) over the frequency range $0.1f_{ce} \leq f < f_{ce}/2$ for LB chorus and $f_{ce}/2 \leq f \leq f_{ce}$ for UB chorus. This wave intensity (V/m) was then averaged over a one second period.

[8] The logarithm of the chorus intensities for upper and lower band chorus is plotted as a function of magnetic latitude as shown in Figures 2b and 2c by the red points, respectively. The chorus is seen to be weak near the magnetic equator and increases exponentially with distance from the equator. An intensity of 10^{-5} V/m indicates the background noise level for each band. A narrowband moving average filter, with bandwidth 15 Hz and 10 ms time resolution, was applied to the center frequency of each chorus band, which was 3.8 kHz for LB chorus and linearly increased from 6.4 to 7.7 kHz for UB chorus. The output of the filter, which was interpolated to fill in the gaps where there were no data from the electric antenna, provides a reasonable fit for each band and is shown by the blue line in Figures 2b and 2c.

[9] For both upper and lower band chorus, the envelope of the intensity near the magnetic equator generally has an exponential dependence on magnetic latitude. An example of this exponential dependence is shown by the solid portion of the black lines in Figure 2b and 2c. This exponential rise within 1° of the magnetic equator can be modeled by $I = I_o e^{\alpha z}$, where I represents intensity, α represents the spatial growth factor, and z represents distance in km from the equator. For this case, the exponential rise near the magnetic equator has $\alpha = 0.97 \times 10^{-3}$ km^{-1} for UB chorus and $\alpha = 0.89 \times 10^{-3}$ km^{-1} for LB chorus.

[10] Surprisingly, in 5 of the 22 events, there was an absence of chorus emissions within 0.5° (~500 km) of the magnetic equator. An example of this behavior is shown in Figure 3a, which displays Cluster 2 observations of banded chorus on September 19, 2003, 03:35:45–03:44:19 for MLT of 11.24 and K_p index of 2+. The data are shown for magnetic latitudes −5° to 0°, with the magnetic equator located at $\lambda_{eq} = -0.17°$. The emissions observed near $\lambda \sim -1°$ appear to be chorus, but do not appear to conform to the banded configuration. Upper and lower chorus bands are observed until the region near the magnetic equator is approached. Outside this zone of exclusion, the chorus intensity is seen to increase with distance away from the magnetic equator.

[11] A number of impulses can be seen in the spectrogram in Figure 3a, some of which are marked by arrows on the time axis. These impulses are artifacts of the automatic gain control (AGC) system of the WBD instrument not updating fast enough. In determining the intensities of each chorus band, each 1-minute spectrogram was also visually inspected. If the emissions appeared to be AGC-produced impulses, they were not included in the integration of the wave spectral density. Therefore, the intensities calculated are only for each band of chorus.

[12] Figures 3b and 3c show in red the logarithm of the chorus intensities for upper and lower band chorus, respectively, with respect to magnetic latitude. An intensity of 10^{-7} V/m indicates the background noise level for each band. For both upper and lower band chorus, the intensity appears to increase with distance away from the magnetic equator. A moving average narrowband filter was applied to the center frequency of each chorus band, which was 6.2 kHz for UB chorus and 4.5 kHz for LB chorus. The output of the filter provides a reasonable fit for each band and is shown as a solid blue line in Figures 3b and 3c. The exponential rise near the magnetic equator, shown by

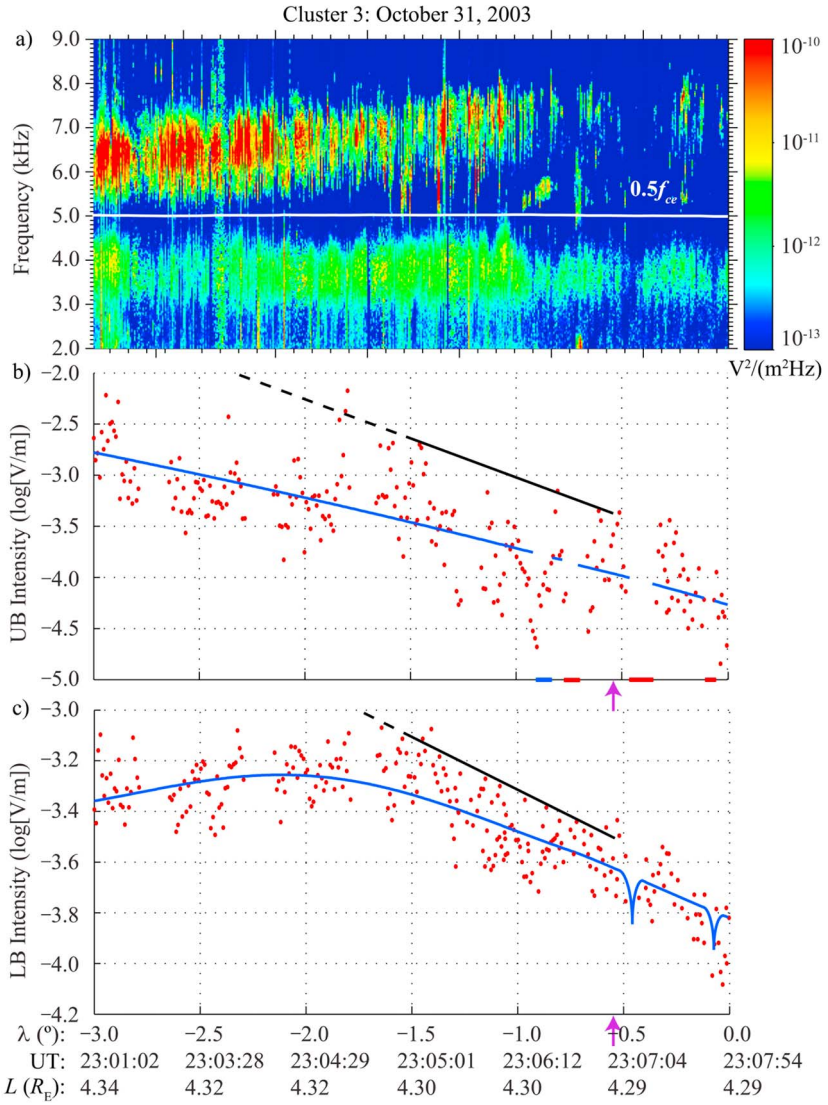

Figure 2. Cluster 3 observations on October 31, 2003 from 23:01:02–23:07:54 UT. (a) E field frequency-time spectrogram showing banded chorus. (b) The logarithm of UB and (c) LB chorus intensity (V/m) as a function of λ is shown in red. Ephemeris data for Cluster 3 is given on the bottom. λ is magnetic dipole latitude in degrees, time in UT, and L is dipole L-shell in R_E. The magnetic equator is located at −0.55°, the MLT is 8.42 h,and the K_p index is 4+.

the solid portion of the black lines in Figures 3b and 3c, has $\alpha = 4.58 \times 10^{-3}$ km^{-1} for UB chorus and $\alpha = 7.18 \times 10^{-3}$ km^{-1} for LB chorus.

3. Spatial Dependence of Chorus Over All Orbits

[13] The two cases from September 19, 2003 and October 31, 2003, shown above, are representative of the entire banded chorus set in this study. The probability of occurrence of different ranges of α for both upper and lower band chorus over all orbits for $\lambda > \lambda_{eq}$ and $\lambda < \lambda_{eq}$ is shown in Figure 4. For both bands of chorus, α has the highest probability of occurrence in the range 0–1 $\times 10^{-3}$ km^{-1} for all λ. This peak probability of occurrence is 64.7% and 72.2% for LB chorus with $\lambda > \lambda_{eq}$ and $\lambda < \lambda_{eq}$, respectively. For UB chorus, this peak probability of occurrence is 61.9% and 40.9% for $\lambda > \lambda_{eq}$ and $\lambda < \lambda_{eq}$, respectively. There is a steep fall in probability from the peak to larger values of α. It appears that α generally has higher values for $\lambda < \lambda_{eq}$ than for $\lambda > \lambda_{eq}$, as seen for $\alpha > 4 \times 10^{-3}$ km^{-1} in Figure 4. However, UB chorus has a much higher probability of occurrence for $\lambda > \lambda_{eq}$ for α in the range 3–4 $\times 10^{-3}$ km^{-1}. The overall distribution of α over all orbits for each band of chorus is approximately exponential.

4. Discussion and Conclusion

[14] For the majority of the chorus cases analyzed, the average intensity of both bands of chorus is exponentially dependent on distance away from the magnetic equator. In our method, the average intensity of the chorus emissions can increase either due to an increase in the number of chorus elements per unit length or due to an intensity increase in each chorus element if the number of elements

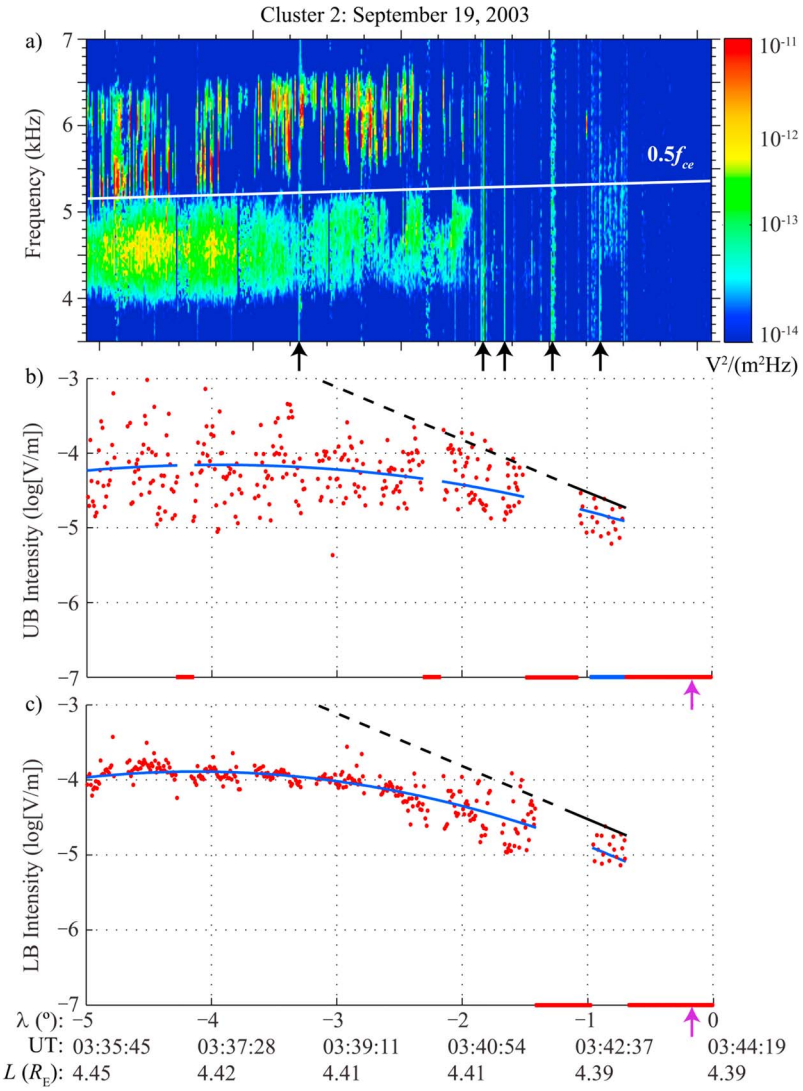

Figure 3. Cluster 2 observations on September 19, 2003 from 03:35:45–03:44:19 UT. (a) E field frequency-time spectrogram showing banded chorus. (b) The logarithm of UB and (c) LB chorus intensity (V/m) as a function of λ is shown in red. Ephemeris data for Cluster 2 is given on the bottom. The magnetic equator is located at −0.17°, the MLT is 11.24 h, and the K_p index is 2+.

per unit length is constant. Though the increase in intensity may be partly due to an increase in number of chorus elements, the majority of the increase in intensity away from the magnetic equator appears to be predominantly due to an increase in intensity of the chorus elements, as seen in Figure 5.

[15] Figure 5a shows observations of two upper band chorus elements from Cluster 3 on October 31, 2003 during 23:07:02–23:07:04 for $\lambda = 0.11°$. On this same day, at a distance further away from the equator at $\lambda = -1.12°$, two much more intense upper band chorus elements are observed in Figure 5b. For this example, the number of chorus elements per unit distance did not increase with distance away from the magnetic equator during the 2 s period of observation, but rather only the intensity of the elements increased.

[16] The similarity of form of the chorus elements suggests that the chorus may be generated at low intensity near

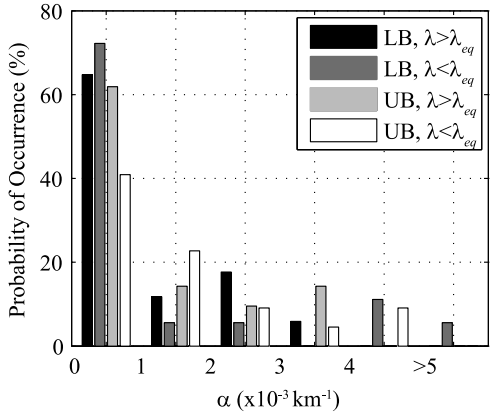

Figure 4. Probability of occurrence of different ranges of spatial growth factor, α, for LB and UB chorus over all orbits.

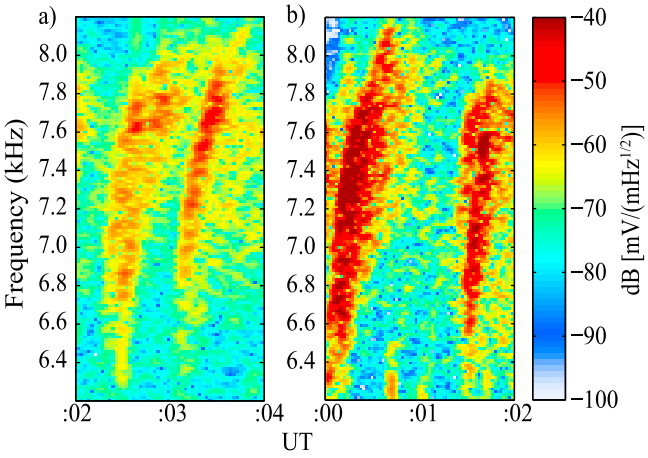

Figure 5. E field frequency-time spectrograms showing Cluster 3 observations of UB chorus on October 31, 2003. (a) Two chorus elements observed during 23:07:02–23:07:04 at $\lambda = 0.11°$. (b) Two much more intense chorus elements observed during 23:06:00–23:06:02 further away from the magnetic equator at $\lambda = -0.12°$.

the magnetic equator, and subsequently amplified to larger intensity as the elements propagate away from the generation point. The amplification mechanism may be linear gyroresonance with energetic electrons. The electron flux, averaged over a pitch angle range of 87.27° to 92.75°, from observations by the PEACE instrument [*Johnstone et al.*, 1997] onboard Cluster 3 on October 31, 2003, seems to provide support for this theory. The particles had energies in the 10–25 keV range, with the highest flux occurring at approximately 1.23° to 1.82° off the magnetic equator.

[17] The average integral electron flux was also calculated for Cluster 3 on October 31, 2003 using RAPID observations for the time interval 23:00–23:15 UT, as seen in Figure 6a, with the location of the magnetic equator shown by the purple arrow. The electron flux is seen to increase significantly during the pass near the magnetic equator, indicating an abundance of electrons for chorus wave growth. This eliminates the possibility that the absence of chorus waves near the magnetic equator is due to *L*-shell rather than λ.

[18] To confirm the location of the magnetic equator, the parallel component of the Poynting vector ($S_{\|}$) normalized by its standard deviation (σ) is shown in Figure 6b for the highest frequency band of the STAFF instrument, 3.63 kHz, which corresponds to approximately the center of the LB chorus. As expected, the parallel component of the Poynting flux turns from negative to positive values near the time when the spacecraft crossed the magnetic equatorial plane. This finding validates the determination of the magnetic equator location using the multipoint method, as it indicates that the waves are propagating away from the equatorial plane.

[19] The previous examples show that for moderate magnetic disturbances, there are 2 main configurations of chorus, one for which there is no chorus present within 0.5° of the magnetic equator and one for which there are only weak chorus emissions present in this region. For either configuration, the envelope of the intensity of banded chorus near the magnetic equator generally has an exponential spatial dependence on distance away from the magnetic equator. This spatial dependence of chorus has not previously been studied or considered in chorus generation models such as those described in *Trakhtengerts* [1999] and *Omura et al.* [2008]. In the *Omura et al.* [2008] model, the growth of the wave amplitude of chorus is studied as a function of time. Initially, this wave growth is found be to linear, after which the wave amplitude grows nonlinearly until it saturates.

[20] The backward wave oscillator (BWO) model [*Trakhtengerts*, 1999] of chorus generation relates this process to an absolute instability of chorus waves, which can occur in the presence of a step-like feature in the electron distribution function. This step-like feature may arise naturally from the cyclotron resonance interaction. It is proposed that electrons with this distribution function move along the magnetic field, usually in regions on the order of 2000 km, and independently generate chorus waves propagating in opposite directions.

[21] The exponential distribution of α provides a new boundary condition for consideration in current and future models of the chorus generation mechanism.

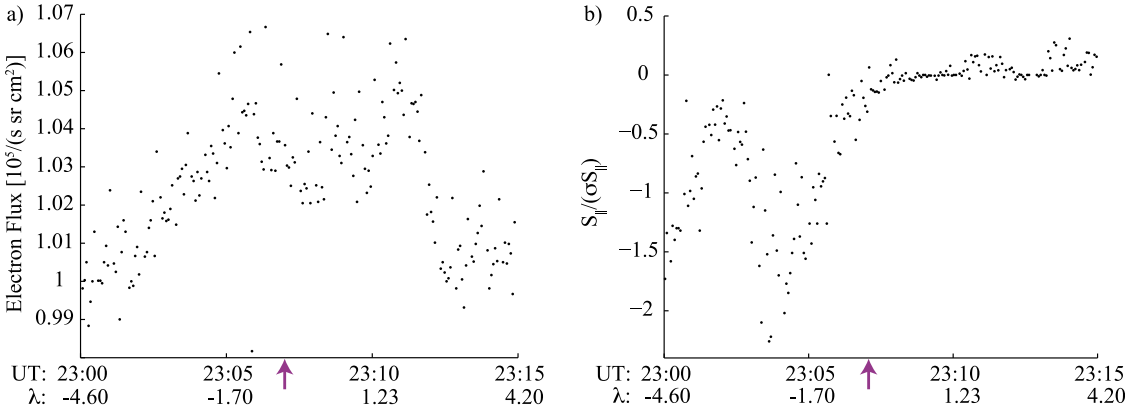

Figure 6. Measurements from Cluster 3 observations on October 31, 2003 during 23:00–23:15 UT with the location of the magnetic equator indicated by the purple arrow. (a) Electron flux and (b) parallel component of the Poynting vector normalized by its standard deviation.

[22] **Acknowledgments.** This research was supported by ONR under parent grant N000140710789 to the University of Maryland, with subcontract Z882802 to Stanford University, and under NASA GSFC grant NNX11AB38G to the University of Iowa.

[23] The Editor thanks Frantisek Nemec and an anonymous reviewer for assisting in the evaluation of this paper.

References

Dunckel, N., and R. A. Helliwell (1969), Whistler-mode emissions on the OGO 1 satellite, *J. Geophys. Res.*, *74*(26), 6371–6385.

Gurnett, D. A., et al. (2001), First results from the Cluster wideband plasma wave investigation, *Ann. Geophys.*, *19*, 1259–1272, doi:10.5194/angeo-19-1259-2001.

Horne, R. B., and R. M. Thorne (1998), Potential waves for relativistic electron scattering and stochastic acceleration during magnetic storms, *Geophys. Res. Lett.*, *25*(15), 3011–3014.

Horne, R. B., R. M. Thorne, S. A. Glauert, J. M. Albert, N. P. Meredith, and R. R. Anderson (2005a), Timescale for radiation belt electron acceleration by whistler mode chorus waves, *J. Geophys. Res.*, *110*, A03225, doi:10.1029/2004JA010811.

Horne, R. B., et al. (2005b), Wave acceleration of electrons in the Van Allen radiation belts, *Nature*, *437*(7056), 227–230, doi:10.1038/nature03939.

Johnstone, A. D., et al. (1997), Peace: A Plasma Electron and Current Experiment, *Space Sci. Rev.*, *79*, 351–398, doi:10.1023/A:1004938001388.

Koons, H. C., and J. L. Roeder (1990), A survey of equatorial magnetospheric wave activity between 5 and 8 R(E), *Planet. Space Sci.*, *38*, 1335–1341, doi:10.1016/0032-0633(90)90136-E.

LeDocq, M. J., D. A. Gurnett, and G. B. Hospodarsky (1998), Chorus source locations from VLF Poynting flux measurements with the POLAR spacecraft, *Geophys. Res. Lett.*, *25*, 4063–4066.

Meredith, N. P., R. B. Horne, and R. R. Anderson (2001), Substorm dependence of chorus amplitudes: Implications for the acceleration of electrons to relativistic energies, *J. Geophys. Res.*, *106*, 13,165–13,178, doi:10.1029/2000JA900156.

Omura, Y., Y. Katoh, and D. Summers (2008), Theory and simulation of the generation of whistler-mode chorus, *J. Geophys. Res.*, *113*, A04223, doi:10.1029/2007JA012622.

Parrot, M. and C. A. Gaye (1994), A statistical survey of ELF waves in a geostationary orbit, *Geophys. Res. Lett.*, *21*, 2463–2466, doi:10.1029/94GL01700.

Russell, C. T., R. E. Holzer, and E. J. Smith (1970), OGO 3 observations of ELF noise in the magnetosphere: 2. The nature of the equatorial noise, *J. Geophys. Res.*, *75*, 755–768, doi:10.1029/JA075i004p00755.

Santolík, O., D. A. Gurnett, J. S. Pickett, J. Chum, and N. Cornilleau-Wehrlin (2009), Oblique propagation of whistler mode waves in the chorus source region, *J. Geophys. Res.*, *114*, A00F03, doi:10.1029/2009JA014586.

Shprits, Y. Y., R. M. Thorne, R. B. Horne, S. A. Glauert, M. Cartwright, C. T. Russell, D. N. Baker, and S. G. Kanekal (2006), Acceleration mechanism responsible for the formation of the new radiation belt during the 2003 Halloween solar storm, *Geophys. Res. Lett.*, *33*, L05104, doi:10.1029/2005GL024256.

Summers, D., B. Ni, and N. P. Meredith (2007a), Timescales for radiation belt electron acceleration and loss due to resonant wave-particle interactions: 1. Theory, *J. Geophys. Res.*, *112*, A04206, doi:10.1029/2006JA011801.

Summers, D., B. Ni, and N. P. Meredith (2007b), Timescales for radiation belt electron acceleration and loss due to resonant wave-particle interactions: 2. Evaluation for VLF chorus, ELF hiss, and electromagnetic ion cyclotron waves, *J. Geophys. Res.*, *112*, A04207, doi:10.1029/2006JA011993.

Thorne, R. M., E. J. Smith, K. J. Fiske, and S. R. Church (1974), Intensity variation of ELF hiss and chorus during isolated substorms, *Geophys. Res. Lett.*, *1*, 193–196, doi:10.1029/GL001i005p00193.

Trakhtengerts, V. Y. (1999), A generation mechanism for chorus emission, *Ann. Geophys.*, *17*, 95–100, doi:10.1007/s005850050739.

Tsurutani, B. E., and E. J. Smith (1974), Postmidnight chorus: A substorm phenomenon, *J. Geophys. Res.*, *79*, 118–127.

Tsurutani, B. T., and E. J. Smith (1977), Two types of magnetospheric ELF chorus and their substorm dependences, *J. Geophys. Res.*, *82*, 5112–5128, doi:10.1029/JA082i032p05112.